International Journal of Chemical, Materials and Biomolecular Sciences
ISSN: 2415-6620
Vol:12, No:2, 2018

Impact of Process Parameters on Tensile Strength of Fused Deposition Modeling Printed Crisscross Poylactic Acid

Shilpesh R. Rajpurohit, Harshit K. Dave

***Abstract*—**Additive manufacturing gains the popularity in recent times, due to its capability to create prototype as well functional as end use product directly from CAD data without any specific requirement of tooling. Fused deposition modeling (FDM) is one of the widely used additive manufacturing techniques that are used to create functional end use part of polymer that is comparable with the injection-molded parts. FDM printed part has an application in various fields such as automobile, aerospace, medical, electronic, etc. However, application of FDM part is greatly affected by poor mechanical properties. Proper selection of the process parameter could enhance the mechanical performance of the printed part. In the present study, experimental investigation has been carried out to study the behavior of the mechanical performance of the printed part with respect to process variables. Three process variables viz. raster angle, raster width and layer height have been varied to understand its effect on tensile strength. Further, effect of process variables on fractured surface has been also investigated.

***Keywords*—**3D printing, fused deposition modeling, layer height, raster angle, raster width, tensile strength.

I. Introduction

IN recent years, additive manufacturing, also known as 3D printing, has tremendous demand due to its ability to create any complex object directly from 3D models. Additive manufacturing has been widely used for rapid prototyping and nowadays it has been shifted from rapid prototyping to rapid manufacturing. Additive manufacturing techniques also has been used to create functional end use product. Additive manufacturing has huge advantages over other processes such as design flexibility, custom designed geometries and low volume production. [1]-[5] Additive manufacturing has been efficiently used in several industries such as automobile, aerospace, medical, electronic and customer product industries [1], [2].

Amongst various additive manufacturing technologies, FDM is foreseen as a widely used additive manufacturing process for prototyping as well end use functional pats. In FDM process, thermoplastic feedstock filament is heated above glass transition temperature and then molten material is extruded through nozzle and deposited on the build table or previously deposited layer as defined by CAD geometry, to create the specimen [1], [2].

Shilpesh R. Rajpurohit is with the S V National Institute of Technology, Surat -395 007 India (e-mail: shilpesh18@gmail.com)

Harshit K. Dave is with the S V National Institute of Technology, Surat – 395 007 India (corresponding author, e-mail: harshitkumar@yahoo.com).

FDM printed part find its application in the automotive, medical aerospace, defense and consumer part industries [5]. However, FDM have some drawbacks including relatively slow process speed, limited accuracy and above all poor mechanical properties of printed parts. The properties of the layered structure of printed part and adhesion between the layers have significant effect on the mechanical properties. Due to huge and promising application of FDM printed parts, their mechanical performance has been subject of much research.

Aliheidari et al. [5] have studied the effect of printing temperature on the fracture resistance and interlayer adhesion of FDM printed ABS material. They observed that fracture resistance of FDM printed ABS material increased with printing temperature. Wang et al. [6] investigated the influence of layer height and bed temperature on the impact strength of Poylactic acid (PLA) part. They observe the higher impact strength at 0.2 m layer height and 160 °C bed temperature over injection molded PLA part due to higher crystallinity. Song et al. [7] studied the mechanical properties of the unidirectional 3D printed PLA part. They observe higher fracture toughness over homogeneous polymer due to crystallinity. During tensile testing, the material is relatively brittle when tested in longitudinal direction than in the transverse direction. Chacon et al. [8] characterized the effect of part orientation, layer height and feed rate on tensile and flexural strength of FDM printed PLA part fabricated using low cost 3D printer. The sample fabricated on edge had optimal mechanical performance in terms of strength, stiffness, and ductility. They also noted down that ductility decreased with increment in layer height. Tensile strength found to be decreased as the feed rate increased in vertically build specimen. Liu et al. [9] applied the Gray Taguchi method to study the influence of the orientation, layer thickness, raster angle, raster width and raster gap on the mechanical properties of the FDM printed PLA parts. They found the deposition orientation and layer thickness was to be significant for all three responses. Uddin et al. [10] evaluated the mechanical properties of FDM printed ABS part with respect to layer thickness, printing plane and printing orientation. Sample printed on edge with smaller layer thickness exhibited higher tensile strength. Carneiro et al. [11] studied the suitability of polypropylene as a printing material while selecting orientation, layer thickness and infill degree as process variable. They found that samples printed in filament direction have higher tensile strength and infill degree has a

significance effect on mechanical properties. Chocklingam et al. [12] optimized tensile strength and density of 3D printed ABS part by suing Non-dominated Sorting Genetic Algorithan (NSGA-2). Motaparti et al. [13] investigated the effect of process variable on flexural properties of fused deposited Ultem 9085 part. They found that vertically build specimens have higher yield strength compared to horizontally build specimen. Negative air gap helps to improve the flexural yield strength. Garg et al. [14] investigate the effect of raster angle on tensile and flexural properties of ABS material. They found that 0° raster angle is the optimum raster angle to achieve higher tensile and flexural strength at lower surface roughness. Syamsuzzaman et al. [15] investigated the effect of layer thickness on tensile and compressive strength of FDM part. They reported that smaller layer thickness with negative air gap could improve the mechanical performance of specimen. Cantrell et al. [16] studied the mechanical properties of FDM printed ABS and PC material using digital image correlation (DIC). They reported that orientation has a significant effect on anisotropy in mechanical properties of ABS and PC part**.** Hill et al. [17] studied the failure criteria for FDM PC material. They reported that failure mechanism is depending on the raster angle and rasters deposited longitudinal to loading direction have higher elongation and strength compared to transversely deposited rasters. Rezayat et al. [18] reported higher tensile strength at 0° raster angle with negative air gap. Riddick et al. [19] reported that the vertically build speciemen has lower tensile strength. Durgun and Ertan [20] found that smaller raster angle has optimal condition for mechanical properties and surface finish. Tanikella et al. [21] found that PC material has higher has higher tensile strength while HIPS has lower tensile strength. Tymark et al. [22] reported that tensile strength obtained by open source 3D printed part is comparable with those printed by commercial 3D printer. Zeimian et al. [23] reported that higher tensile strength obtained at 0° raster angle followed by ±45°, 45° and 0° raster angle.

Some work has been carried out to study the mechanical properties of FDM printed parts. However, mechanical performance of FDM printed parts is not fully explored yet. Mechanical performance of the parts is crucible to use it as functional end use part. Mechanical performance of the printed part is significantly affected by selection of printing variables. To the best of the author's knowledge, there is limited study which has been reported on effect of printing variables on the mechanical performance of printed parts and fracture behaviors of parts. Hence, there is requirement of to study the effect of process variable on mechanical performance of printed parts.

In the present study, effect of process variable has been carried out on tensile properties of 3D printed PLA parts. To this end, tensile specimens of PLA were designed and 3D printed by selecting layer height, raster width and raster angle as process variable. The effect of process variables on fracture surface was also investigated

II. Experimental Details

A. Fabrication of Tensile Specimen

ASTM D638 is the most common standard used for tensile characterization of 3D printed polymer parts. PLA is semi crystalline and environmental friendly feedstock material with excellent printing capability, and thus it is very popular among 3D printer community. Therefore, PLA was selected as the model material. PLA filament feedstock with 1.75 mm diameter was used in an Omega dual extruder printer, to fabricate the tensile specimens with a Slic3r software.

The geometry and dimensions of the tensile specimen were shown in Fig. 1.

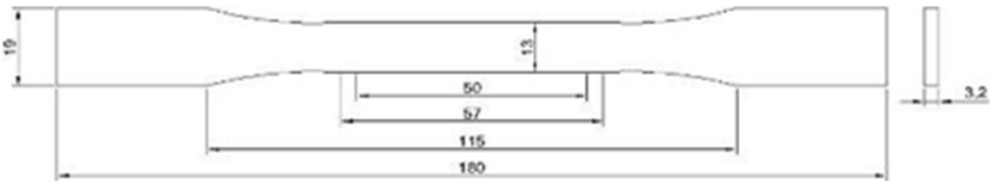

Fig. 1 Tensile specimen as per ASTM D638

The tensile specimens were printed at the three different levels of the raster angle, layer height and raster width. The PLA filament was extruded at 210 °C from the printer nozzle as a semi molten material and deposited on to print bed, which was maintained at 70 °C. A 100% infill density has been used with rectilinear pattern with one perimeter to print the specimens. Upon completion, sharp blade has been used to remove the spacemen from the build plate. The printing conditions are summarized in Table I.

In the present investigation, full factorial experimental design has been used to perform experimental run. Three factors have been varied at the three levels so according to full factorial experimental design, total 27 number of experiments have been performed as shown in Table II.

TABLE I
FDM 3D Printing Condition

Process parameter	Value
Raster angle (°) (variable)	0/90, 30/60, 45/45
Layer height (µm) (variable)	100, 200, 300
Raster width (µm) (variable)	400, 500, 600
Liquefier temperature (°C)	210
Bed temperature (°C)	70
No. of perimeters	1
Infill percentage (%)	100
Infill pattern	Rectilinear

B. Tensile Testing

The tensile specimens prepared by above method were loaded for tensile testing till the specimen fracture using Tinius Olsen H50KL universal testing machine as shown in Fig. 2. The tests were conducted under controlled displacement at a constant crosshead speed of 5 mm/min. The machine had a load cell of 50 kN and built in horizon and the software allows to control, monitor and record measurement data. The experimental results of the tensile strength have been shown in Table II.

Fig. 2 Experimental setup for tensile testing

TABLE II
TENSILE STRENGTH OF FDM PRINTED PLA

Sr. No.	Raster angle (°)	Layer height (µm)	Raster width (µm)	Tensile strength (MPa)
1	0/90	100	400	32.9
2	0/90	100	500	44.9
3	0/90	100	600	41.7
4	0/90	200	400	33.1
5	0/90	200	500	52.0
6	0/90	200	600	42.4
7	0/90	300	400	31.0
8	0/90	300	500	43.2
9	0/90	300	600	47.6
10	30/60	100	400	24.9
11	30/60	100	500	47.5
12	30/60	100	600	45.6
13	30/60	200	400	25.8
14	30/60	200	500	52.5
15	30/60	200	600	41.2
16	30/60	300	400	37.0
17	30/60	300	500	52.9
18	30/60	300	600	53.7
19	45/45	100	400	40.1
20	45/45	100	500	51.4
21	45/45	100	600	35.5
22	45/45	200	400	23.8
23	45/45	200	500	50.8
24	45/45	200	600	41.3
25	45/45	300	400	34.7
26	45/45	300	500	53.8
27	45/45	300	600	54.2

III. RESULTS AND DISCUSSION

By using Taguchi method, experimental design converts the response values to S/N ratio, which is known as quality characteristic evaluation index. With the help of S/N ratio, the least variations and optimal quality design can be obtained. The objective of the present investigation is to maximize the tensile strength of the part. Therefore, the larger the better characteristics are used. The experimental results of tensile strength in S/N ratio have been shown in Table III. Furthermore, the Analysis of Variance (ANOVA) can be adopted to identify the significance of each process variable and interactions on the tensile strength of test specimen. Relative information of process variables and interactions could be determined by ANOVA, and the ANOVA results have been presented in Table IV.

TABLE III
S/N RATIO FOR TENSILE STRENGTH

Sr. No.	Raster angle (°)	Layer height (µm)	Raster width (µm)	S/N ratio
1	0/90	100	400	30.3439
2	0/90	100	500	33.0449
3	0/90	100	600	32.4027
4	0/90	200	400	30.3966
5	0/90	200	500	34.3201
6	0/90	200	600	32.5473
7	0/90	300	400	29.8272
8	0/90	300	500	32.7097
9	0/90	300	600	33.5521
10	30/60	100	400	27.9240
11	30/60	100	500	33.5339
12	30/60	100	600	33.1793
13	30/60	200	400	28.2324
14	30/60	200	500	34.4032
15	30/60	200	600	32.2979
16	30/60	300	400	31.3640
17	30/60	300	500	34.4691
18	30/60	300	600	34.5995
19	45/45	100	400	32.0629
20	45/45	100	500	34.2193
21	45/45	100	600	31.0046
22	45/45	200	400	27.5315
23	45/45	200	500	34.1173
24	45/45	200	600	32.3190
25	45/45	300	400	30.8066
26	45/45	300	500	34.6156
27	45/45	300	600	34.6800

The optimum level of three process variables for tensile strength can be obtained intuitively from the main effect plot for S/N ratio as shown in Fig. 3. Optimum process variable levels with significant process variables and interactions for the tensile strength have been shown in Table V.

A. Effect of Raster Angle

As shown in Fig. 3, at 45°/45° raster angle highest tensile strength has been observed followed by 30°/60° and 0°/90° raster angle. The stress-strain curve for different raster angle has been shown in Fig. 4. It can be noted that, at 45°/45° raster

angle higher tensile strength has been observed, while higher elongation has been obtained with 30°/60° raster angle and low elongation has been observed with 0°/90° raster angle.

TABLE IV
ANOVA FOR TENSILE STRENGTH

Source	DF	SS	MS	F-value	P-value
Raster angle	2	0.276	0.1382	0.12	0.892
Layer height	2	7.079	3.5397	2.96	0.109
Raster width	2	82.682	41.3411	34.59	0.000
Raster angle × Layer height	4	6.712	1.6781	1.40	0.316
Raster angle × Raster width	4	4.018	1.0046	0.84	0.537
Layer height × Raster width	4	7.582	1.8956	0.84	0.537
Error	8	9.560	1.1950		
Total	26	117.911			

Fig. 5 shows the fractured surface of the specimen at different raster angle. At 45°/45° raster angle, layers have been deposited at 45° to the loading direction then next layer deposited with a 90° increment to the previously deposited layer. The bonding between the layer and within the layer has been found to be very effective which increases the tensile strength of the part. It can be seen that, for 0°/90° raster angle, half of the layers are deposited longitudinal to loading direction and half of the layers are deposited transverse to loading direction. So, half of the layers pulled through the longitudinal direction, but the remaining layers have been pulled through the bonding between adjacent beads, which lowers the strength of the parts.

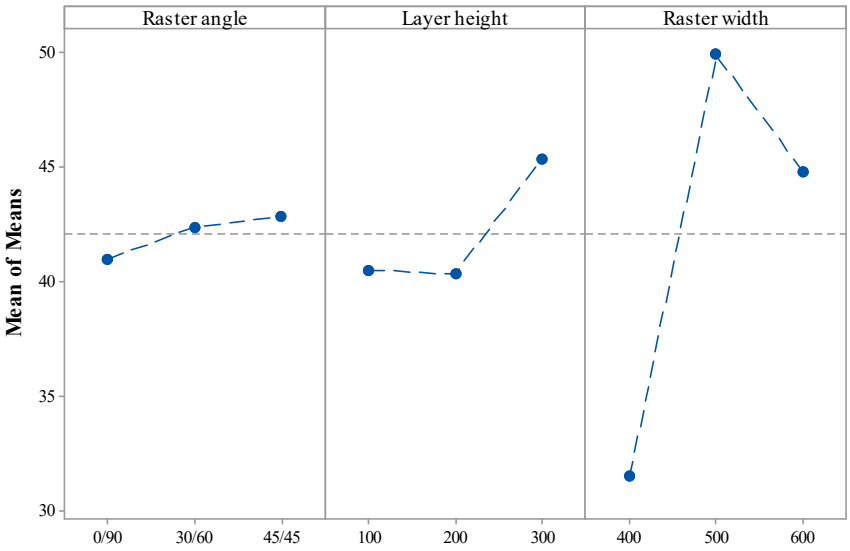

Fig. 3 Main effect plot of S/N ratio for tensile strength

TABLE V
OPTIMUM PROCESS VARIABLE LEVEL WITH SIGNIFICANT VARIABLES

Process variables	Level	Values
Raster angle	1	45°/45°
Layer height	3	300 µm
Raster width	2	500 µm
Significant variable	Raster width	

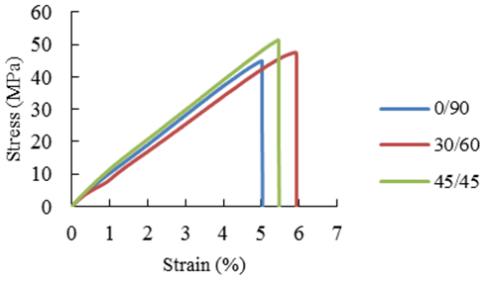

Fig. 4 Stress-strain curve for different raster angle

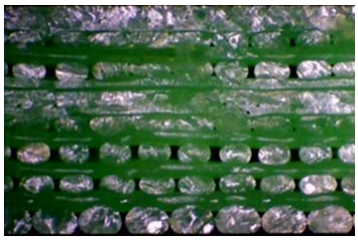

(a)

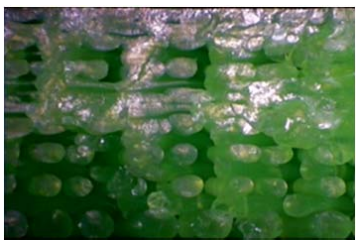

(b)

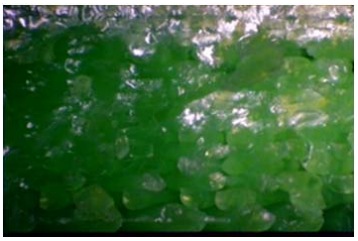

(c)

Fig. 5 Fractured surface of specimen at (a) 0°/90°, (b) 30°/60° and (c) 45°/45° raster angle

B. Effect of Layer Height

As shown in Fig. 3, at 300 µm layer height, higher tensile strength has been obtained. The stress-strain curve for different layer height has been shown in Fig. 6. It can be seen that, at 100 µm layer height, lower strength has been observed with less elongation, while higher strength has been observed at 300 µm layer height with more elongation of the specimen.

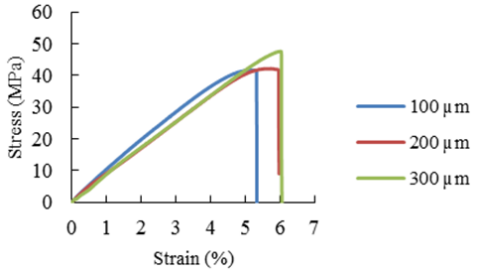

Fig. 6 Stress-strain curve for different layer height

Fig. 7 shows the fractured surface of the specimen at different layer height. It can be seen that at 200 µm layer height, voids between the deposited beads have been observed, which reduces strength of the specimen. On the other hand, at 300 µm layer height, more bonding has been observed between the adjacent deposited bead ultimately, which enhances the load bearing capacity results into higher strength.

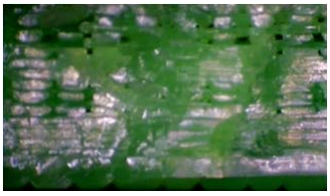

(a)

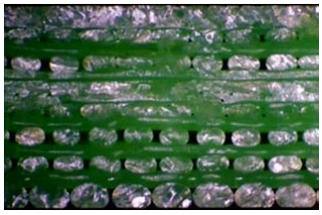

(b)

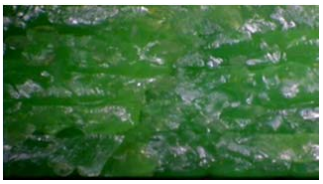

(c)

Fig. 7 Fractured surface of specimen at (a) 100 µm, (b) 200 µm and (c) 300 µm layer height

C. Effect of Raster Width

As shown Fig. 3, at 200 µm layer height, higher tensile strength has been obtained. The stress-strain curve for different raster width has been shown in Fig. 8. It can be seen that lower tensile strength with higher elongation has been observed at 400 µm raster width, while higher tensile has been achieved at 500 µm raster width at the loss of elongation.

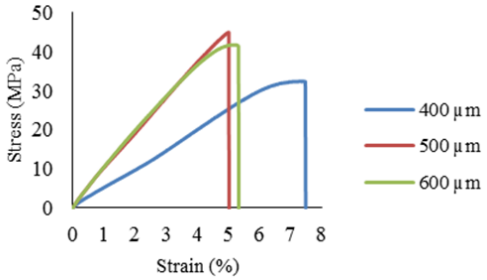

Fig. 8 Stress-strain curve for different raster width

Fig. 9 shows the fractured surface of the specimen at different raster width. It can be seen that higher number of voids at 400 µm raster width reduces the bonding between the beads results into lesser strength. At 500 µm raster width, less voids have been observed so that higher amount of necking has been formed between beads. Higher amount of necking improves the bonding between the deposited beads so that more load can be borne by beads, that results into higher strength.

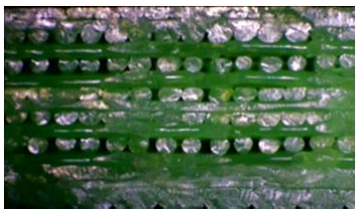

(a)

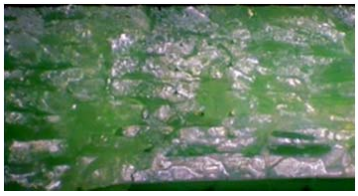

(b)

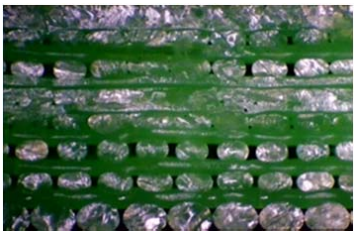

(c)

Fig. 9 Fractured surface of specimen at (a) 400 µm, (b) 500 µm and (c) 600 µm raster width

IV. Conclusions

In the present study, tensile strength has been selected to characterize the mechanical performance of the 3D printed PLA part. The full factorial set of three process variable with three levels was designed, and the Taguchi method was used to optimize and study the influence of various process variables. ANOVA has been carried out in order to find the significant process variables. Furthermore, analysis of fractured surface has been carried out to understand the fracture behavior of specimen. Based on experimental results, the following conclusions can be drawn.

- 45°/45° raster angle has higher tensile strength followed by 30°/60° and 0°/90° raster angle.
- Higher tensile strength has been found at the higher value of the layer height.
- At 500 µm raster width, higher tensile strength has been observed and raster angle is found to be significant process variable affecting strength.
- Voids have been observed during microscopic examination of the fractured surface that may cause to reduce the tensile strength.

References

[1] C. K. Chua, K. F. Leong, 3D printing and additive manufacturing: principles and applications of rapid prototyping, World Scientific Publishing Co Inc., 2014.
[2] I. Gibson, D. W. Rosen, B. Stucker, Additive manufacturing technologies, New York: Springer, 2010.
[3] R. D. Goodridge, M. L. Shofner, R. J. M. Hague, M. McClelland, M. R. Schlea, R. B. Johnson, and C. J. Tuck, "Processing of a olyamide-12/carbon nanofibre composite by laser sintering," Polymer Testing, vol. 30, 2011, pp. 94-100.
[4] M. Baumers, P. Dickens, C. Tuck, and R. Hague, "The cost of additive manufacturing: machine productivity, economies of scale and technology-push," Technol. Forecast. Soc. Change, vol. 102, 2016, pp. 193-201.
[5] N. Aliheidari, R. Tripuraneni, A. Ameli, and S. Nadimpalli, "Fracture resistance measurement of fused deposition modeling 3D printed polymers," Polymer Testing, vol. 60, 2017, pp. 94-101.
[6] L. Wang, W. M. Gramlich, and D. J. Gardner, "Improving the impact strength of Poly (lactic acid) (PLA) in fused layer modeling (FLM)," Polymer, vol. 114, 2017, pp. 242-248.
[7] Y. Song, Y. Li, W. Song, K. Yee, K. Y. Lee, and V. L. Tagarielli, "Measurements of the mechanical response of unidirectional 3D-printed PLA," Materials & Design, vol. 123, 2017, pp. 154-164.
[8] J. M. Chacón, M. A. Caminero, E. García-Plaza, and P. J. Núñez, "Additive manufacturing of PLA structures using fused deposition modelling: Effect of process parameters on mechanical properties and their optimal selection," Materials & Design, vol. 124, 2017, pp. 143-157.
[9] X. Liu, M. Zhang, S. Li, L. Si, J. Peng, and Y. Hu, "Mechanical property parametric appraisal of fused deposition modeling parts based on the gray Taguchi method," The International Journal of Advanced Manufacturing Technology, vol. 89, 2017, pp. 2387-2397.
[10] M. S. Uddin, M. F. R. Sidek, M. A. Faizal, R. Ghomashchi, and A. Pramanik, "Evaluating Mechanical Properties and Failure Mechanisms of Fused Deposition Modeling Acrylonitrile Butadiene Styrene Parts. Journal of Manufacturing Science and Engineering," vol. 139, 2017, pp.081018-1-12
[11] O. S. Carneiro, A. F. Silva, and R. Gomes, "Fused deposition modeling with polypropylene," Materials & Design, vol. 83, 2015, pp. 768-776.
[12] K. Chockalingam, N. Jawahar, and J. Praveen, "Enhancement of anisotropic strength of fused deposited ABS parts by genetic algorithm" Materials and Manufacturing Processes, vol. 31, 2016, pp. 2001-2010.
[13] K. P. Motaparti, G. Taylor, M. C. Leu, K. Chandrashekhara, J. Castle, and M. Matlack, "Experimental investigation of effects of build parameters on flexural properties in fused deposition modelling parts," Virtual and Physical Prototyping, 2017, pp. 1-14.
[14] A. Garg, A. Bhattacharya, and A. Batish, "Failure investigation of fused deposition modelling parts fabricated at different raster angles under tensile and flexural loading," Proceedings of the Institution of Mechanical Engineers, Part B: Journal of Engineering Manufacture, vol. 231, 2017, pp. 2031-2039.
[15] M. Syamsuzzaman, N. A. Mardi, M. Fadzil, and Y. Farazila, "Investigation of layer thickness effect on the performance of low-cost and commercial fused deposition modelling printers," Materials Research Innovations, vol. 18, 2014, pp. S6-485.
[16] J. Cantrell, S. Rohde, D. Damiani, R. Gurnani, L. DiSandro, J. Anton, A. Young, A. Jerez, D. Steinbach, C. Kroese, and P. Ifju, "Experimental Characterization of the Mechanical Properties of 3D Printed ABS and Polycarbonate Parts," In Advancement of Optical Methods in Experimental Mechanics, vol. 3, 2017, pp. 89-105.
[17] N. Hill, and M. Haghi, "Deposition direction-dependent failure criteria for fused deposition modeling polycarbonate," Rapid Prototyping Journal, vol. 20, 2014, pp. 221-227.
[18] H. Rezayat, W. Zhou, A. Siriruk, D. Penumadu, and S. S. Babu, "Structure–mechanical property relationship in fused deposition modelling," Materials Science and Technology, vol. 31, 2015, pp. 895-903.
[19] J. C. Riddick, M. A. Haile, R. Von Wahlde, D. P. Cole, O. Bamiduro, and T. E. Johnson, "Fractographic analysis of tensile failure of acrylonitrile-butadiene-styrene fabricated by fused deposition modeling," Additive Manufacturing, vol. 11, 2016, pp. 49-59.
[20] I. Durgun, and R. Ertan, "Experimental investigation of FDM process for improvement of mechanical properties and production cost," Rapid Prototyping Journal, vol. 20, 2014, pp. 228-235.
[21] N. G. Tanikella, B. Wittbrodt, and J. M. Pearce, "Tensile strength of commercial polymer materials for fused filament fabrication 3D printing," Additive Manufacturing, vol. 15, 2017, pp. 40-47.
[22] B. M. Tymrak, M. Kreiger, and J. M. Pearce, "Mechanical properties of components fabricated with open-source 3-D printers under realistic environmental conditions," Materials & Design, vol. 58, 2014, pp. 242-246.
[23] S. Ziemian, M. Okwara, and C. W. Ziemian, "Tensile and fatigue behavior of layered acrylonitrile butadiene styrene," Rapid Prototyping Journal, vol. 21, 2015, pp. 270-278